International Journal of Biological Macromolecules 158 (2020) 819–825

Contents lists available at ScienceDirect

International Journal of Biological Macromolecules

journal homepage: http://www.elsevier.com/locate/ijbiomac

Voltammetric detection of miRNA hybridization based on electroactive indicator-cobalt phenanthroline

Arzum Erdem [a,b,*], Ece Eksin [a], Gulce Kadikoylu [a,b], Esma Yildiz [a,b]

[a] Analytical Chemistry Department, Faculty of Pharmacy, Ege University, 35100, Bornova, Izmir, Turkey
[b] Biomedical Technologies Department, Graduate School of Natural and Applied Sciences, Ege University, 35100, Bornova, Izmir, Turkey

ARTICLE INFO

Article history:
Received 7 February 2020
Received in revised form 18 April 2020
Accepted 21 April 2020
Available online 24 April 2020

Keywords:
microRNA
Electroactive indicator
Electrochemical miRNA biosensor
Pencil graphite electrode
Cobalt phenanthroline

ABSTRACT

The indicator-based nucleic acid detection protocol is one of the major approaches to monitor the sequence-selective nucleic acid hybridization-mediated recognition events in biochemical analysis. The metal complex, cobalt phenanthroline, $[Co(phen)_3^{3+}]$, which is one of the electroactive indicators, interacts more with double stranded nucleic acids via intercalation. Thus, this interaction permits an increase at the electrochemical signal of $[Co(phen)_3^{3+}]$. In our study, the interaction of metal complex, $[Co(phen)_3^{3+}]$ with nucleic acids was examined using pencil graphite electrodes (PGEs) in combination with differential pulse voltammetry (DPV) technique. The voltammetric detection of miRNA-34a was investigated based on the changes at the electrochemical signal of $[Co(phen)_3^{3+}]$ under optimized experimental conditions; such as accumulation potentialof metal complex and DNA probe concentration, hybridization time, target miRNA concentration. Furthermore, the selectivity of electrochemical miRNA-34a biosensor was studied in contrast to different miRNAs. The applicability of indicator-based biosensor specific to miRNA-34a was also presented by using total RNA samples.

© 2020 Elsevier B.V. All rights reserved.

1. Introduction

Biosensors are devices capable of identifying by means of their biological receptor, which can convert this recognition into a signal with a converter. Due to the high selectivity and specificity of biosensors, it is the reason of choice in the determination and analysis of environmental, food, medicine fields [1–6]. In recent years, DNA biosensors, which have gained an important place in DNA diagnosis and biological studies, have been increasing their role in recognizing specific DNA sequences. DNA sensors in chip, crystal and electrode forms are biorecognizers that are sensitive to surface changes, have high sensitivity in hybridization and interaction formation and have rapid analysis [3,4,7].

The use of electrochemical DNA biosensors in medical conditions such as diagnosis, analysis and monitoring has increased. The important reasons of this demand are compared to traditional methods; high sensitivity, cost-effective, fast and accurate measurements [8]. Due to the simplicity, low cost and high sensitivity of electrochemical biosensors, the demand for this method has increased over time [3,4,7–9]. There are important points in the principle of the electrochemical DNA biosensor. The stability and amount of single-strand DNA probe immobilized is important and also the stability and interaction of the target DNA sequence to the probe [8,10,11]. Ensuring the stability of the DNA-transducer surface connection and increasing the amount of DNA immobilized are particularly important in electrochemical DNA biosensor improvement studies [8,12]. Sequence-specific DNA hybridization analysis can be examined by determining of the oxidation signal of the DNA bases, adenine and guanine, or signal generated by the electroactive compounds, or electroactive complexes which have high affinity to DNA [13–26]. In order to determine the hybridization, it is common to use a redox indicator which is capable of recognizing the hybrid at the surface via its electrochemical. In indicator-based detection, the difference between the affinity of the indicator to the single-strand and double-strand oligonucleotide is used as an evidence of hybridization. Indicators are more likely to bind to double strand oligonucleotides, due to their ability yo bind to the grooves on the duplex DNA sequence [3]. One of these indicators is the metal complex, cobalt 1,10-phenanthroline, also known as electrochemical indicator [27]. Recent studies have shown that transition metal complexes assume a biologically important role. In particular, 1,10-phenanthroline (phen) compounds have been shown to inhibit tumor growth after interaction with DNA. Related to this subject, the role of metal complexes in the design of drugs, reactive probes, diagnostic reagents and understanding of

* Corresponding author at: Ege University, Faculty of Pharmacy, Analytical Chemistry Department, Bornova, 35100 Izmir, Turkey.
E-mail address: arzum.erdem@ege.edu.tr (A. Erdem).

https://doi.org/10.1016/j.ijbiomac.2020.04.168
0141-8130/© 2020 Elsevier B.V. All rights reserved.

the DNA interaction of these complexes are of curiosity. The use of such electroactive metal complexes in the development of new anti-cancer drugs may form a new approach [27].

microRNAs (miRNAs) are approximately 22-nucleotide non-coding RNAs, which regulate gene expression and play a pivotal role in tumorigenesis. miRNA-34a acts as a tumor-suppressor gene in multiple malignancies by targeting many oncogenes related to proliferation, apoptosis and invasion. In addition, miRNA-34a is a significant biomarker in colon cancer, prostate, breast, lung, kidney, bladder, pancreatic carcinomas [28,29].

In the present study, the metal complex, cobalt phenanthroline, [Co(phen)$_3^{3+}$], which is an electroactive indicator was used for the first time to detect nucleic acid hybridization related to miRNA by using DPV method in combination with PGE. The experimental conditions, such as; accumulation potential of metal complex and DNA probe concentration, hybridization time, target miRNA concentration were optimized based on the changes observed at the reduction signal of [Co(phen)$_3^{3+}$]. The selectivity of the indicator-based biosensor was explored against to different miRNA sequences. The applicability of voltammetric biosensor to detect miRNA-34a was also shown in total RNA samples.

2. Material and method

2.1. Apparatus

DPV measurements were performed using the AUTOLAB-PGSTAT 302 electrochemical analysis system and GPES 4.9 software package (Eco Chemie, The Netherlands). Voltammetric measurements were performed with triple electrode system, PGE was used as working electrode, Ag/AgCl/3M KCl (BAS, Model RE-5B, W. Lafayette, USA) was used as reference electrode and platinum wire was used as auxiliary electrode. All measurements were performed in the faraday cage at room temperature.

2.2. Chemicals

DNA probes and complementary RNA oligonucleotides (ODN), were purchased (as lyophilized powder) from TIB Molbiol (Germany). The base sequences of ODNs are listed below:

miR 34a DNA Probe: 5′-Amino-C_6-ACA ACC AGC TAA GAC ACT GCC A-3′.

miR 34a Target: 5′-UGG CAG UGU CUU AGC UGG UUG U-3′ (U: uracil).

Mismatch of miR 34a (MM): 5′-UGG CAG U**A**U CU**A** AGC UGG UUG U-3′ .

Noncomplementary RNA (NC): 5′-AUG CAU GCA UGC AUG CAU GCA A-3′.

All nucleic acid sequences were prepared in 50 mM phosphate buffer containing 20 mM NaCl (PBS, pH 7.40).

The synthesis of [Co(phen)$_3^{3+}$] was performed as reported in earlier studies [13]. The stock solution of [Co(phen)$_3^{3+}$] was prepared in 1 mM concentration by dissolving in 20 mM Tris-HCl buffer with 20 mM NaCl (TBS, pH 7.00) in an ultrasonic water bath for 5 min and then, it was diluted to 0.2 mM concentration before use.

2.3. Isolation of total RNA from cell lysates

The isolation of total RNA from human hepatocellular carcinoma cell line (HUH-7) was performed as reported in our earlier study [30].

2.4. Procedure

The whole procedure followed for the developed biosensor consists of four steps as depicted in Fig. 1.

(i) The electrochemical activation of PGE.
(ii) The hybridization of the probe with its complementary miRNA-34a target, or with non-complementary sequences (NC), or two-base mismatch (MM) at the PGE surface.
(iii) The accumulation of the metal complex, [Co(phen)$_3^{3+}$], onto PGE surface, or miRNA-34a probe immobilized PGE or hybrid immobilized PGE.
(iv) The voltammetric measurements.

All steps are carried out at room temperature.

2.5. Electrode preparation

Tombow HB 0.5 mm pencil lead (Japan) that was held on the Rotring Pencil model (Germany) was used as an electrode. The electrochemical

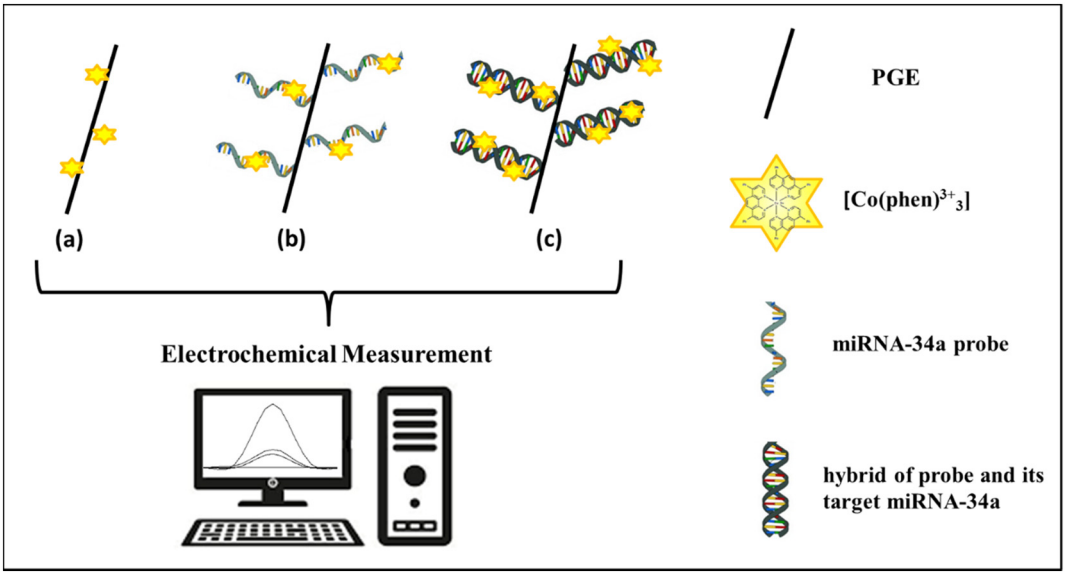

Fig. 1. The representative scheme of the experimental procedure. (a) [Co(phen)$_3^{3+}$] accumulation onto (a) PGE surface, (b) miRNA-34a probe immobilized PGE, (c) hybrid immobilized PGE followed by electrochemical measurement.

activation of the surface of each electrode was done by applying a potential of +1.40 V for 30 s in acetate buffer (ABS, pH, 4.80) via DPV [31]. The electrochemical activation of the electrode surface by applying the potential helps to form –COOH groups at the surface while increasing the hydrophilicity of the surface and the active sites of the electrode [32].

2.6. Hybridization of DNA probe with its target miRNA-34a/NC/MM

PGEs were immersed into the 100 μL of 0.25 μg/mL (36.8 nM) miRNA-34a probe in PBS (pH 7.40) during 30 min. The immobilization of miRNA-34a probe onto electrode surface was performed by covalent coupling between carboxylic groups of PGE surface and amino group linkage at the 5′ end of miRNA-34a probe [33]. Then, probe immobilized electrodes were rinsed with PBS to inhibit unspecific binding onto the electrode surface.

Probe immobilized PGEs were immersed into the vials containing 100 μL miRNA-34a target for hybridization process by using passive adsorption for 30 min. After the hybrid occurrence onto the surface, PGEs were rinsed with PBS before $[Co(phen)_3^{3+}]$ accumulation.

2.7. Total RNA analysis

Total RNA isolated from HUH-7 cell line was diluted to final target concentration in PBS (pH, 7.40) and probe immobilized PGEs were immersed into the vials containing 100 μL target for enabling hybridization for 30 min and hybrid immobilized PGEs were washed in PBS (pH, 7.40) before $[Co(phen)_3^{3+}]$ accumulation.

2.8. Accumulation of $[Co(phen)_3^{3+}]$

Accumulation of the $[Co(phen)_3^{3+}]$ was performed onto the surfaces of bare PGE, DNA probe immobilized PGE and hybrid immobilized PGE. Accumulation was performed by applying +0.2 V during 180 s using magnetic stirrer. After accumulation of $[Co(phen)_3^{3+}]$, the electrode was rinsed with TBS (pH, 7.00) for 5 s. The reduction signal of $[Co(phen)_3^{3+}]$ was then measured by DPV technique.

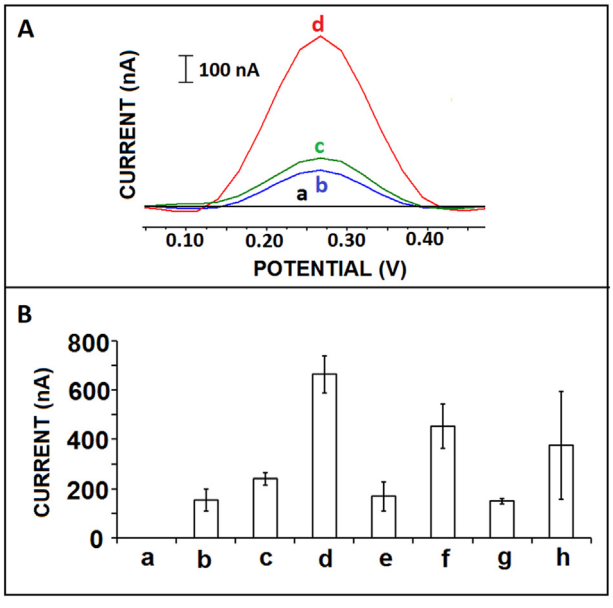

Fig. 2. (A) DPVs related to a) the control experiment in TBS, reduction signal of $[Co(phen)_3^{3+}]$ after accumulation onto b) PGE, c) probe. immobilized PGE, d) hybrid covered PGE. (B) Bar graphs representing (a) the signal obtained in control experiment in the medium of buffer and the average signal of $[Co(phen)_3^{3+}]$ ($n = 3$) onto (b) PGE, (c) before and (d) after hybridization of 0.25 μg/mL (36.8 nM) miRNA-34a probe with its target, (e) before and (f) after hybridization of 0.5 μg/mL (73.5 nM) miRNA-34a probe with its target, (g) before and (h) after hybridization of 1 μg/mL (147 nM) miRNA-34a probe with its target.

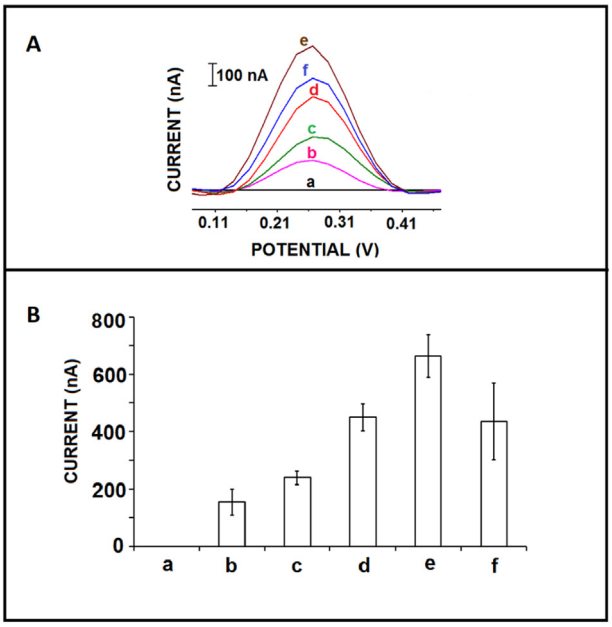

Fig. 3. DPVs and bar graphs representing a) the control experiment in TBS, the average reduction signal of $[Co(phen)_3^{3+}]$ after accumulation onto (b) PGE, c) probe. immobilized PGE, reduction signal of $[Co(phen)_3^{3+}]$ after hybridization of miRNA-34a probe with its target during d) 15 min, e) 30 min, f) 60 min hybridization (n = 3).

2.9. Electrochemical Measurement

The reduction signal of $[Co(phen)_3^{3+}]$ was measured in TBS (pH 7.00). DPV measurements were performed by scanning between +0.6 V to -—0.2 V at the pulse amplitude 100 mV with a scan rate 50 mV/s and step potential of 25 mV. The raw data were treated using the Savitzky and Golay filter (level 2) of the GPES software (Eco Chemie, The Netherlands), followed by the moving average baseline correction, using a “peak width” of 0.03.

3. Results and discussion

Firstly, the experimental parameters; such as, probe concentration, hybridization time and target concentration were optimized before

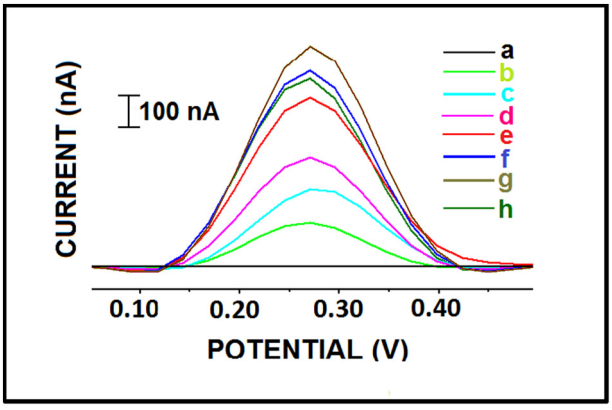

Fig. 4. DPVs representing a) the control experiment in TBS, the average reduction signal of $[Co(phen)_3^{3+}]$ after accumulation onto (b) PGE, c) probe. immobilized PGE, reduction signal of $[Co(phen)_3^{3+}]$ after hybridization of miRNA-34a probe and (d) 1 μg/mL (142.3 nM), (e) 2 μg/mL (284.6 nM), (f) 3 μg/mL (426.9 nM), (g) 4 μg/mL (569.1 nM) and (h) 5 μg/mL (711.4 nM) miRNA-34a target.

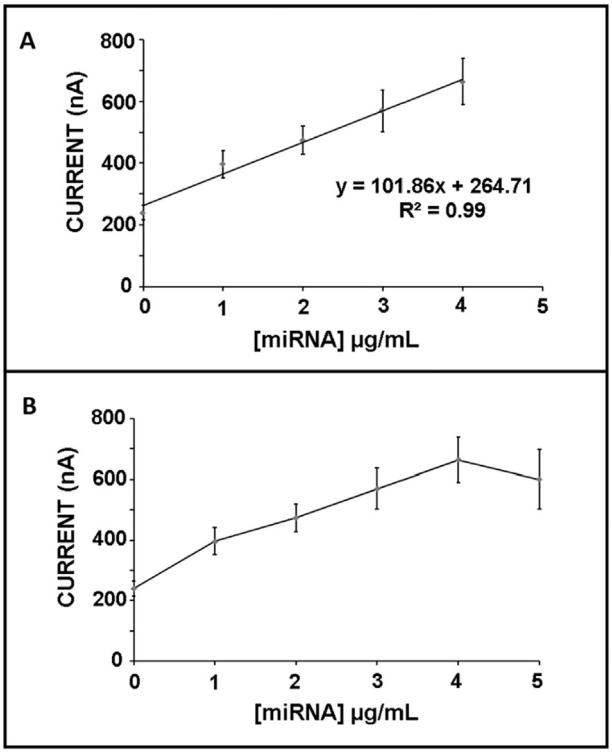

Fig. 5. (A) Calibration plot related to the average reduction signal of $[Co(phen)_3^{3+}]$ after accumulation onto the surface of PGE in case of hybridization of probe with its miRNA-34a at different concentrations from 1 to 4 µg/mL (142.3 nM to 569.1 nM) (n = 3). (B) Line plot related to the average reduction signal of $[Co(phen)_3^{3+}]$ after accumulation onto the surface of PGE in case of hybridization between probe and miRNA-34a at its different concentrations from 1 to 5 µg/mL (142.3 nM to 711.4 nM) (n = 3).

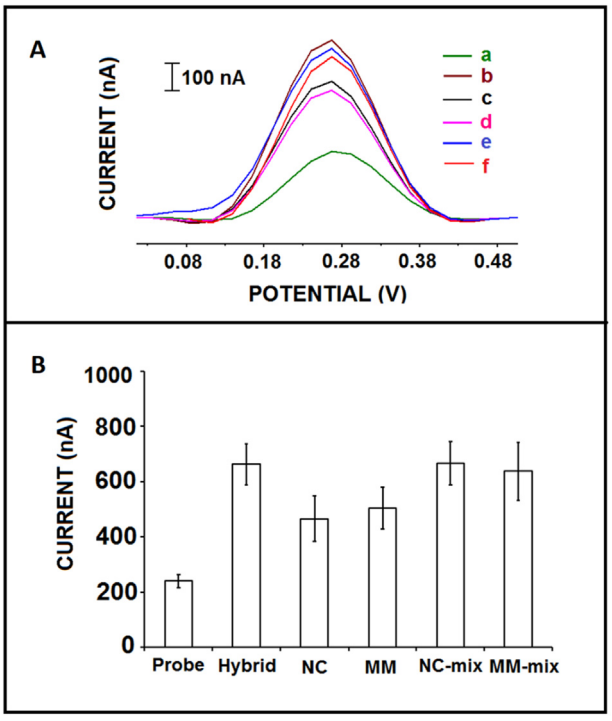

Fig. 6. DPVs and bar graphs representing the reduction signal of $[Co(phen)_3^{3+}]$ after accumulation onto the surface of a) probe immobilized PGE, after hybridization of probe and b) miRNA-34a, c) NC, d) MM, the mixture of e) miRNA-34a and NC, f) miRNA34a and MM (n = 3).

voltammetric detection of miRNA. The detection method relies on the magnitude of the peak of $[Co(phen)_3^{3+}]$ that reflects the extent of the hybrid formation [11,13,34]. The dependence of the peak current of $[Co(phen)_3^{3+}]$ on the accumulation potential was also studied. For this purpose, $[Co(phen)_3{}^{3+}]$ was accumulated onto the PGE surface by applying + 0.2 V or + 0.5 V during 3 min, or applying without any potential. The highest value of $[Co(phen)_3^{3+}]$ signal was obtained as 190.25 ± 53.66 nA (RSD %, 28.20%, $n = 3$) when + 0.2 V potential was applied. Therefore, + 0.2 V was chosen as optimum accumulation potential for further studies.

In this present study, the reduction signal of $[Co(phen)_3^{3+}]$ is measured in the absence/presence of miRNA-34a probe and after solid phase hybridization between probe and its complementary target. The increase ratio (%) is calculated between the signal recorded by probe immobilized PGE and the signal that obtained by hybrid covered PGE. The highest increase ratio (%) indicated the optimum condition. Note that, during the calculations the reduction signal of $[Co(phen)_3{}^{3+}]$ in the absence of probe and hybrid is omitted.

The effect of miRNA-34a probe concentration upon the hybridization was then investigated (Fig. 2). The hybridization was performed between 4 µg/mL (569.1 nM) miRNA-34a target and miRNA-34a probe at different concentration level from 0.25 µg/mL (36.8 nM) to 1 µg/mL (147 nM). After accumulation of $[Co(phen)_3^{3+}]$ onto the surface

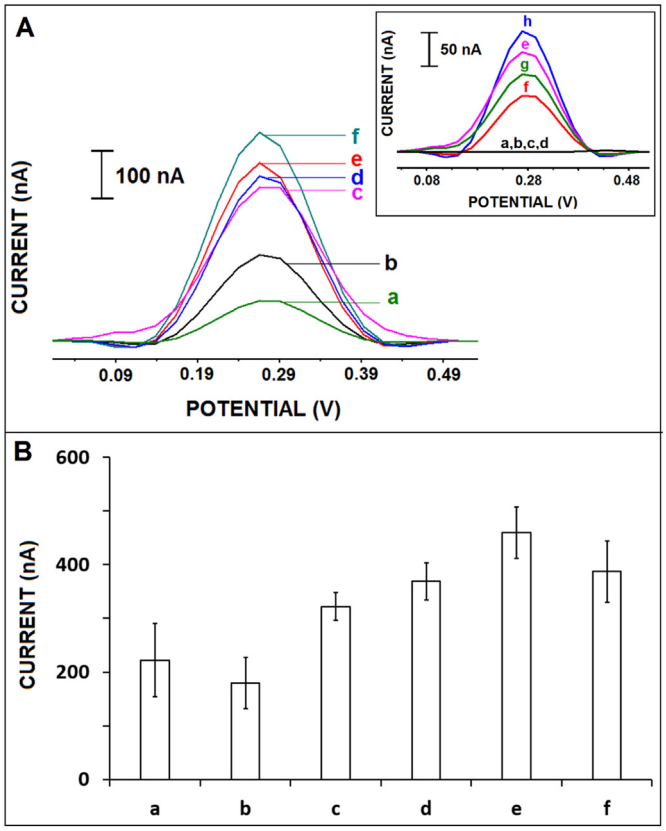

Fig. 7. (A) DPVs (B) Bar graphs representing the average reduction signal (n = 3) of $[Co(phen)_3^{3+}]$ after accumulation onto the surface of probe. immobilized PGE (a) in the absence of total RNA and miRNA-34a target, (b) in the presence of 1 µg/mL total RNA and after hybridization between probe and miRNA-34a spiked into total RNA medium in the various concentration of miRNA-34a; (c) 1 µg/mL, (d) 2 µg/mL, (e) 3 µg/mL, (f) 4 µg/mL. Inset figure: DPVs representing the control experiment in the absence of $[Co(phen)_3^{3+}]$ (a) in the absence of probe and total RNA sample, (b) probe immobilized PGE in the absence of total RNA, (c) total RNA immobilized PGE in the absence of probe, (d) probe immobilized PGE in the presence of 1 µg/mL total RNA, and the reduction signal of $[Co(phen)_3^{3+}]$ after its accumulation onto the surface of (e) PGE in the absence of probe and total RNA immobilization, (f) probe immobilized PGE in the absence of total RNA, (g) total RNA immobilized PGE in the absence of probe, (h) probe immobilized PGE in the presence of 1 µg/mL total RNA.

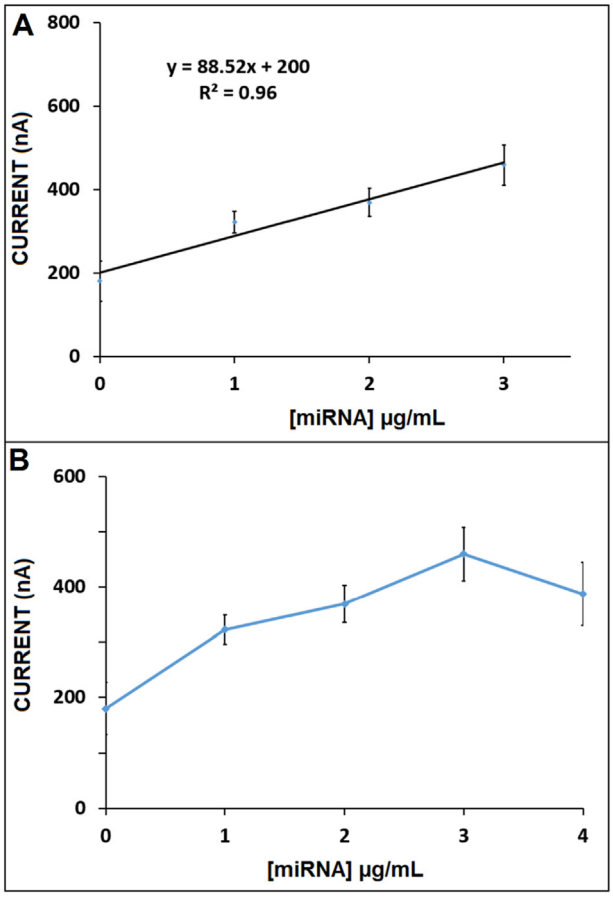

Fig. 8. (A) Calibration plot related to the average reduction signal (n = 3) of $[Co(phen)_3^{3+}]$ measured in the presence of hybridization between probe and miRNA-34a target spiked into the total RNA medium at different concentrations of miRNA-34a from 1 to 3 µg/mL (142.3 nM to 426.9 nM). (B) Line plot related to the average reduction signal (n = 3) of $[Co(phen)_3^{3+}]$ measured after hybridization of probe with miRNA-34a spiked into the total RNA medium at different concentrations of miRNA-34a from 1 to 4 µg/mL (142.3 nM to 569.1 nM).

of 0.25 µg/mL (36.8 nM), 0.5 µg/mL (73.5 nM) and 1 µg/mL (147 nM) probe immobilized PGE, the signal was measured as 240.10 ± 24.07 nA, 169.50 ± 60.10 nA and 150 ± 9.89 nA, respectively. The low peak current indicated that $[Co(phen)_3^{3+}]$ has a very weak binding affinity to a single-stranded probe sequence via electrostatic interaction at the electrode surface. A significant increase at the signal was observed after hybridization of DNA probe with its complementary target miRNA. There is an increase (i.e 2.5–2.8 fold) obtained at the signal after the hybridization occured between probe and 4 µg/mL of miRNA in various concentrations of probe from 0.25 µg/mL to 1 µg/mL (36.8 nM to 147 nM) probe. This increase at the response is a proof that the detection of miRNA hybridization could be investigated based on the response of electroactive indicator, $[Co(phen)_3^{3+}]$. Since the highest increase at the response of metal complex was recorded after miRNA hybridization of 0.25 µg/mL (36.8 nM) probe with 4 µg/mL (569.1 nM) target as 663.14 ± 74.50 nA (RSD %, 11.23%, $n = 3$), 0.25 µg/mL (36.8 nM) probe concentration was chosen as optimum probe concentration for further studies.

Secondly, the hybridization of 0.25 µg/mL (36.8 nM) probe and 4 µg/mL (569.1 nM) target was performed during 15, 30 and 60 min hybridization time (Fig. 3). The average signal was measured as 240.1 ± 24.07 nA (RSD %, 10.02%, $n = 3$) after accumulation of $[Co(phen)_3^{3+}]$ onto the surface of 0.25 µg/mL (36.8 nM) probe immobilized PGE. There was 87.42%, 176.19% and 81.31% increase observed at the signal after the hybridization of miRNA-34a probe with its target during 15, 30 and 60 min, respectively. The highest increase at the signal was obtained in case of 30 min hybridization time (i.e, measured as 663.14 ± 74.50 nA with a RSD %, 11.23%, $n = 3$) shown in Fig. 3-e. Thus, 30 min hybridization time was chosen as optimum for further studies.

The effect of target concentration upon to the response of indicator-based biosensor was also studied. It could be seen from Fig. 4 that there was an increase at the peak current of $[Co(phen)_3^{3+}]$ while increasing miRNA concentration from 1 µg/mL to 4 µg/mL (142.3 nM to 569.1 nM). In Fig. 5A, there was a linear correlation between the peak current and miRNA concentration with a regression equation of $y = 101.86x + 264.71$ and a linear regression coefficient of 0.99. The detection limit [35] was calculated and found to be 0.59 µg/mL (83.9 nM), which was comparable to the ones reported in earlier studies [33,36–39].

In the case of hybridization of probe with 5 µg/mL (711.4 nM) target miRNA-34a, a lower signal was obtained in comparison to the one

Table 1
The comparison of our assay to some of earlier reports presenting electrochemical detection of miRNA.

Electrode	miRNA	Method	DL	Real Sample	Analysis Time	Reference
IL-CA-PGE	miRNA-34a	DPV	0.56 µg/mL in PBS 0.40 µg/mL in FBS 0.88 µg/mL in total RNA medium	+	35 min	[30]
GO/CA/PGE		EIS	1.12 µg/mL in PBS 0.29 µg/mL in FBS	+	125 min	[36]
CNFs/SPE		DPV, EIS	10.98 µg/mL	−	50 min	[37]
PPy-PGE		CV, EIS	0.20 µg/mL	+	40 min	[41]
GO/CA/PGE		DPV	7.52 µg/mL	−	200 min	[38]
IL/CA/PGE		EIS	0.772 µg/mL	+	150 min	[39]
GO/PGE		CV, EIS	1.9 µg/mL	+	90 min	[33]
MWCNT-GCE		DPV	1 pM	+	65 min	[42]
Os(VI)bipy-HMDE	miRNA-522	DPV	2 nM	−	85 min	[43]
MoS_2-Thi-AuNPs nanocomposite/GCE	miRNA-21	SWV	0.26 pM	+	18 h	[44]
Gold disk electrode	let 7a	DPV	1 nM	−	24 h 40 min	[45]
Gold electrode	miRNA-145	EIS, SWV	0.37 fM	−	18 h	[46]
CB/PGE MWCNTs/PGE GO/PGE	miRNA-125a	EIS	0.01 nM 1 nM 0.1 nM	+	2 h 35 min	[47]
PGE	miRNA-34a	DPV	0.59 µg/mL (83.9 nM) in PBS 0.79 µg/mL (112.3 nM) in total RNA medium	+	65 min	This study

obtained with 4 μg/mL (569.1 nM) miRNA-34a (Fig. 5B). Therefore, 4 μg/mL (569.1 nM) miRNA-34a was chosen as the saturation point of the probe immobilized PGE. Thus, 4 μg/mL (569.1 nM) was chosen for selectivity studies.

The sensitivity of the PGE was then calculated from the ratio of the slope of the calibration plot (shown in Fig. 5A), and the active surface area of working electrode; thus, the sensitivity value was found to be 0.296 μA nM^{-1} cm^{-2}.

In order to demonstrate the selectivity of the indicator-based biosensor, the hybridization was performed between miRNA-34a probe and different miRNA sequences as non-complementary miRNA (NC) and two-base mismatch miRNA (MM). Additionally, the selectivity of the sensor is tested in mixture samples; mixture of miR34-a target and NC or mixture of miRNA-34a target and MM (Fig. 5).

After full hybridization of miRNA-34a probe and its complementary target, peak current of [$Co(phen)_3{}^{3+}$] was measured as 663.14 ± 74.50 nA (RSD%, 11.23%, $n = 3$). (Fig. 6-b). When NC was used, a lower peak current was recorded (Fig. 6-c). The selectivity of biosensor towards to MM was also studied. The selectivity experiments showed that miRNA biosensor presents a high selectivity to proper sequence-selective detection of microRNAs even in the presence of microRNAs having a different single-base differentiation.

Regarding to the application of our assay, total RNA samples were used in order to show the applicability of indicator based-miRNA biosensor to real samples. Under the optimized conditions, the solid phase hybridization was performed in different concentrations of miRNA-34a target spiked into the medium of total RNA sample. Accordingly, the detection of miRNA-34a spiked into the total RNA sample was investigated by means of measuring the reduction signal of [$Co(phen)_3^{3+}$] before and after hybridization.

As in the case of synthetic oligonucleotides, a low reduction signal was observed before hybridization due to low affinity interaction of [$Co(phen)_3^{3+}$] to single stranded nucleic acids. There was a linear increase at current response in the concentration range of miRNA-34a target from 1 μg/mL to 3 μg/mL (142.3 nM to 426.9 nM) that was spiked into total RNA sample (Fig. 7). In the case of hybridization between probe and 4 μg/mL (569.1 nM) miRNA-34a, the average signal of indicator is recorded as 459.66 ± 48.26 nA (RSD%, 10.50%, $n = 3$), which was lower the than the one obtained with 3 μg/mL (426.9 nM) miRNA-34a (shown in Fig. 8).

In the previous study related to the effect of miRNA-34a concentration upon to biosensor response in buffer media, the highest signal of indicator was observed with 4 μg/mL miRNA-34a. However of this fact, the highest signal is observed with 3 μg/mL (426.9 nM) miRNA-34a spiked into total RNA medium. Accordingly, these results indicate that specific detection of miRNA-34a could be successfully even it is spiked into the real sample matrix like total RNA sample.

The detection limit was calculated based on the method described by Miller and Miller [35] and found to be 0.79 μg/mL (112.3 nM) in total RNA medium.

4. Conclusion

An electrochemical microRNA biosensor based on the disposable pencil graphite electrode (PGEs) was utilized herein for detection of microRNA-34a which is well-known biomarker for different cancer types [28,29]. Herein, the PGEs provide more rapid and practical detection process comparison to other electrodes, such as gold electrode [17], carbon paste electrode [34] and glassy carbon electrode [40].

In comparison to the earlier studies (summarized in Table 1), our microRNA sensing platform exhibited some advantages such as being cost-effective, single-use, easy-to-handle and being portable. Based on an electroactive indicator, metal complex [$Co(phen_3^{3+})$], our assay yields lower detection limits, as 0.59 μg/mL (83.9 nM) in buffer and 0.79 μg/mL (112.3 nM) in total RNA medium that were much lower than the ones in earlier studies related to miRNA analysis without applying any surface modification of electrode by using (nano)materials such as; GO, CNF or IL [30,33,36–39]. Our assay provides a short detection protocol and does not require any pre-amplification or, purification steps. In addition, the results claim that miRNA biosensor could be applied successfully to miRNA detection in real samples.

Acknowledgements

Authors acknowledge to Dr. Bekir Cetinkaya for the synthesis of [$Co(phen)_3(ClO_4)_3$] and to Dr. Yasemin Erac for kindly providing total RNA sample from Human hepatocellular carcinoma cell line (HUH-7). A.E. would like to express her gratitude to the Turkish Academy of Sciences (TUBA) as a Principal member for its partial support.

References

[1] J.C. Cooper, E.A.H. Hall, The nature of biosensor technology, J. Biomed. Eng. 10 (1988) 210–219, https://doi.org/10.1016/0141-5425(88)90001-5.
[2] P. Mehrotra, Biosensors and their applications–a review, J. Oral Biol. Craniofac. Res. 6 (2016) 153–159.
[3] J. Wang, Electrochemical nucleic acid biosensors, Anal. Chim. Acta 469 (2002) 63–71, https://doi.org/10.1016/S0003-2670(01)01399-X.
[4] M. Trotter, N. Borst, R. Thewes, F. von Stetten, Review: electrochemical DNA sensing – principles, commercial systems, and applications, Biosens. Bioelectron. 154 (2020), 112069. https://doi.org/10.1016/j.bios.2020.112069.
[5] L.D. Mello, L.T. Kubota, Review of the use of biosensors as analytical tools in the food and drink industries, Food Chem. 77 (2002) 237–256, https://doi.org/10.1016/S0308-8146(02)00104-8.
[6] K.R. Rogers, Biosensors for environmental applications, Biosens. Bioelectron. 10 (1995) 533–541, https://doi.org/10.1016/0956-5663(95)96929-S.
[7] A. Erdem, M. Ozsoz, Nucleic acids as biorecognition element in biosensor development, in: M. Mascini, I. Palchetti (Eds.), Nucleic Acid Biosensors for Environmental Pollution Monitoring, Royal Society of Chemistry, UK 2011, pp. 17–33.
[8] F. Li, Y. Feng, P. Dong, B. Tang, Gold nanoparticles modified electrode via a mercaptodiazoaminobenzene monolayer and its development in DNA electrochemical biosensor, Biosens. Bioelectron. 25 (2010) 2084–2088, https://doi.org/10.1016/j.bios.2010.02.004.
[9] S. Liu, J. Liu, X. Han, Y. Cui, W. Wang, Electrochemical DNA biosensor fabrication with hollow gold nanospheres modified electrode and its enhancement in DNA immobilization and hybridization, Biosens. Bioelectron. 25 (2010) 1640–1645, https://doi.org/10.1016/j.bios.2009.11.026.
[10] K.B. Cederquist, R.S. Golightly, C.D. Keating, Molecular beacon—metal nanowire Interface: effect of probe sequence and surface coverage on sensor performance, Langmuir 24 (2008) 9162–9171, https://doi.org/10.1021/la703854x.
[11] T.H. Kjällman, H. Peng, C. Soeller, J. Travas-Sejdic, Effect of probe density and hybridization temperature on the response of an electrochemical hairpin-DNA sensor, Anal. Chem. 80 (2008) 9460–9466, https://doi.org/10.1021/ac801567d.
[12] S.F. Liu, Y.F. Li, J.R. Li, L. Jiang, Enhancement of DNA immobilization and hybridization on gold electrode modified by nanogold aggregates, Biosens. Bioelectron. 21 (2005) 789–795, https://doi.org/10.1016/j.bios.2005.02.001.
[13] A. Erdem, B. Meric, K. Kerman, T. Dalbasti, M. Ozsoz, Detection of interaction between metal complex indicator and DNA by using electrochemical biosensor, Electroanalysis 11 (1999) 1372–1376, https://doi.org/10.1002/(SICI)1521-4109(199912)11:18<1372::AID-ELAN1372>3.0.CO;2-4.
[14] C. Ding, F. Zhao, M. Zhang, S. Zhang, Hybridization biosensor using 2, 9-dimethyl-1, 10-phenantroline cobalt as electrochemical indicator for detection of hepatitis B virus DNA, Bioelectrochemistry 72 (2008) 28–33, https://doi.org/10.1016/j.bioelechem.2007.11.001.
[15] A. Erdem, K. Kerman, B. Meric, U.S. Akarca, M. Ozsoz, DNA electrochemical biosensor for the detection of short DNA sequences related to the hepatitis B virüs, Electroanalysis 11 (1999) 586–587, https://doi.org/10.1002/(SICI)1521-4109(199906)11:8<586::AID-ELAN586>3.0.CO;2-J.
[16] A. Erdem, H. Karadeniz, P.E. Canavar, G. Congur, Single-use sensor platforms based on carbon nanotubes for electrochemical detection of DNA hybridization related to Microcystis spp, Electroanalysis 24 (2012) 502–511, https://doi.org/10.1002/elan.201100369.
[17] H. Karadeniz, B. Gulmez, A. Erdem, F. Jelen, M. Ozsoz, E. Palecek, Echinomycin and cobalt-phenanthroline as redox indicators of DNA hybridization at gold electrodes, Front. Biosci. 11 (2006) 1870–1877, https://doi.org/10.2741/1930.
[18] A., Erdem, K., Kerman, B. Meric, M. Ozsoz, Methylene Blue as a novel electrochemical hybridization indicator. Electroanalysis 13 (2001219–223. (10.1002/1521-4109(200103)13:3<219::AID-ELAN219>3.0.CO;2-7).
[19] A. Ferancová, M. Adamovski, P. Gründler, J. Zima, J. Barek, J. Mattusch, J. Labuda, Interaction of tin (II) and arsenic (III) with DNA at the nanostructure film modified electrodes, Bioelectrochemistry. 71 (2007) 33–37. doi:https://doi.org/10.1016/j.bioelechem.2006.07.013.
[20] S. Arounaguiri, D. Easwaramoorthy, A. Ashokkumar, A. Dattagupta, B.G. Maiya, Cobalt (III), nickel (II) and ruthenium (II) complexes of 1, 10-phenanthroline family of ligands: DNA binding and photocleavage studies, J. Chem. Sci. 112 (2000) 1–17, https://doi.org/10.1007/BF02704295.

[21] Q. Wang, Y. Ding, L. Wang, J. Ni, Z. Yu, H. Lin, F. Gao, Low-background, highly sensitive DNA biosensor by using an electrically neutral cobalt (II) complex as the redox hybridization indicator, Chem. Asian J. 8 (2013) 1455–1462, https://doi.org/10.1002/asia.201300047.
[22] M.V. Del Pozo, C. Alonso, F. Pariente, E. Lorenzo, Electrochemical DNA sensing using osmium complexes as hybridization indicators, Biosens. Bioelectron. 20 (2005) 1549–1558, https://doi.org/10.1016/j.bios.2004.08.002.
[23] M.V. Del Pozo, C. Alonso, F. Pariente, E. Lorenzo, DNA biosensor for detection of helicobacter pylori using phen-dione as the electrochemically active ligand in osmium complexes, Anal. Chem. 77 (2005) 2550–2557, https://doi.org/10.1021/ac0489263.
[24] K.M. Millan, S.R. Mikkelsen, Sequence-selective biosensor for DNA based on electroactive hybridization indicators, Anal. Chem. 65 (1993) 2317–2323, https://doi.org/10.1021/ac00065a025.
[25] S. Karastogianni, S. Girousi, Detection of short oligonucleotide sequences of hepatitis B virus using electrochemical DNA hybridisation biosensor, Chem. Pap. 69 (2015) 202–210, https://doi.org/10.2478/s11696-014-0599-6.
[26] X.M. Li, H.Q. Ju, C.F. Ding, S.S. Zhang, Nucleic acid biosensor for detection of hepatitis B virus using 2,9-dimethyl-1,10-phenanthroline copper complex as electrochemical indicator, Anal. Chim. Acta 582 (2007) 158–163, https://doi.org/10.1016/j.aca.2006.09.004.
[27] S. Niu, F. Li, S. Zhang, L. Wang, X. Li, S. Wang, Studies on the interaction mechanism of 1, 10-phenanthroline cobalt (II) complex with DNA and preparation of electrochemical DNA biosensor, Sensors 6 (2006) 1234–1244, https://doi.org/10.3390/s6101234.
[28] X.J. Li, Z.J. Ren, J.H. Tang, MicroRNA-34a: a potential therapeutic target in human cancer, Cell Death Dis. 5 (2014) e1327, https://doi.org/10.1038/cddis.2014.270.
[29] G. Misso, M.T. Di Martino, G. De Rosa, A.A. Farooqi, A. Lombardi, V. Campani, M. Caraglia, Mir-34: a new weapon against cancer? Mol. Ther. Nucleic Acids 3 (2014) e195, https://doi.org/10.1038/mtna.2014.47.
[30] E. Yaralı, E. Kanat, Y. Erac, A. Erdem, Ionic liquid modified single-use electrode developed for voltammetric detection of mi RNA-34a and its application to real samples, Electroanalysis 32 (2019) 384–393, https://doi.org/10.1002/elan.201900353.
[31] E. Eksin, D. Polat, A. Erdem, Voltammetric and Impedimetric detection of interaction between Dacarbazine and nucleic acids, Electroanalysis 31 (2019) 2012–2019, https://doi.org/10.1002/elan.201900284.
[32] G. Cui, J.H. Yoo, J.S. Lee, J. Yoo, J.H. Uhm, G.S. Cha, H. Nam, Effect of pre-treatment on the surface and electrochemical properties of screen-printed carbon paste electrodes, Analyst 126 (2001) 1399–1403, https://doi.org/10.1039/b102934g.
[33] G. Congur, E. Eksin, A. Erdem, Impedimetric detection of microRNA at graphene oxide modified sensors, Electrochim. Acta 172 (2015) 20–27, https://doi.org/10.1016/j.electacta.2015.03.210.
[34] A. Erdem, K. Kerman, B. Meric, U.S. Akarca, M. Ozsoz, Novel hybridization Indicator methylene blue for the electochemical detection of short DNA sequences related to the hepatitis B virus, Anal. Chim. Acta 422 (2000) 139–149, https://doi.org/10.1016/S0003-2670(00)01058-8.
[35] J.N. Miller, J.C. Miller, Statistics and Chemometrics for Analytical Chemistry, 5th ed England Pearson Prentice Hall, Harlow, 2005.
[36] A. Erdem, E. Eksin, D. Isin, D. Polat, Graphene oxide modified chemically activated graphite electrodes for detection of microRNA, Electroanalysis 29 (2017) 1350–1358, https://doi.org/10.1002/elan.201600761.
[37] A. Erdem, E. Eksin, G. Congur, Indicator-free electrochemical biosensor for microRNA detection based on carbon nanofibers modified screen printed electrodes, J. Electroanal. Chem. 755 (2015) 167–173, https://doi.org/10.1016/j.jelechem.2015.07.031.
[38] D. Isin, E. Eksin, A. Erdem, Graphene oxide modified single-use electrodes and their application for voltammetric miRNA analysis, Mater. Sci. Eng. C. 75 (2017) 1242–1249, https://doi.org/10.1016/j.msec.2017.02.166.
[39] E. Kesici, E. Eksin, A. Erdem, An Impedimetric biosensor based on ionic liquid-modified graphite electrodes developed for microRNA-34a detection, Sensors 18 (2018) E2868, https://doi.org/10.3390/s18092868.
[40] X. Li, L. Yang, X. Li, S. Yan, Y. Ren, M. Wang, P. Liu, Y. Dong, C. Zhang, $[Cu(phen)_2]^{2+}$ acts as electrochemical indicator and anchor to immobilize probe DNA in electrochemical DNA biosensor, Anal. Biochem. 492 (2016) 56–62, https://doi.org/10.1016/j.ab.2015.09.011.
[41] J. Mandli, A. Amine, Impedimetric genosensor for miRNA-34a detection in cell lysates using polypyrrole, J. Solid State Electrochem. 22 (2018) 1007–1014, https://doi.org/10.1007/s10008-017-3819-5.
[42] F. Li, J. Peng, J. Wang, H. Tang, L. Tan, Q. Xie, S. Yao, Carbon nanotube-based label-free electrochemical biosensor for sensitive detection of miRNA-24, Biosens. Bioelectron. 54 (2014) 158–164, https://doi.org/10.1016/j.bios.2013.10.061.
[43] M. Bartosik, M. Trefulka, R. Hrstka, B. Vojtesek, E. Palecek, Os (VI) bipy-based electrochemical assay for detection of specific microRNAs as potential cancer biomarkers, Electrochem. Commun. 33 (2013) 55–58, https://doi.org/10.1016/j.elecom.2013.04.009.
[44] D. Zhu, W. Liu, D. Zhao, Q. Hao, J. Li, J. Huang, L. Wang, Label-free electrochemical sensing platform for microRNA-21 detection using thionine and gold nanoparticles co-functionalized MoS2 nanosheet, ACS Appl. Mater. Interfaces 9 (2017) 35597–35603, https://doi.org/10.1021/acsami.7b11385.
[45] N. Xia, X. Wang, D. Deng, G. Wang, H. Zhai, S.J. Li, Label-free electrochemical sensor for MicroRNAs detection with ferroceneboronic acids as redox probes, Int. J. Electrochem. Sci. 8 (2013) 9714–9722, https://doi.org/10.1002/elan.201300077.
[46] P. Jolly, M.R. Batistuti, A. Miodek, P. Zhurauski, M. Mulato, M.A. Lindsay, P. Estrela, Highly sensitive dual mode electrochemical platform for microRNA detection, Sci. Rep. 6 (2016), 36719. https://doi.org/10.1038/srep36719.
[47] G. Yammouri, J. Mandli, H. Mohammadi, A. Amine, Development of an electrochemical label-free biosensor for microRNA-125a detection using pencil graphite electrode modified with different carbon nanomaterials, J. Electroanal. Chem. 806 (2017) 75–81, https://doi.org/10.1016/j.jelechem.2017.10.012.